

AN INVESTIGATION OF NUCLEATE BOILING
FROM MESH COVERED SURFACES

Francis Carl Gregory

United States Naval Postgraduate School



THE S I S

AN INVESTIGATION OF NUCLEATE BOILING
FROM MESH COVERED SURFACES

by

Francis Carl Gregory

June 1970

*This document has been approved for public re-
lease and sale; its distribution is unlimited.*

T133833

LIBRARY
NAVAL POSTGRADUATE SCHOOL
MONTEREY, CALIF. 93940

An Investigation of Nucleate Boiling
From Mesh Covered Surfaces

by

Francis Carl Gregory
Lieutenant, United States Navy
B.S., United States Naval Academy, 1963

Submitted in partial fulfillment of the
requirements for the degree of

MASTER OF SCIENCE IN MECHANICAL ENGINEERING

from the

NAVAL POSTGRADUATE SCHOOL
June 1970

ABSTRACT

A boiler apparatus, designed to simulate heat pipe operation, was built and used to investigate nucleate boiling at atmospheric pressure from mesh covered surfaces using distilled water as the working fluid. The wick materials used included 50 mesh, 80 mesh, and 150 mesh nickel screen; 100 count Lektromesh, a one-piece electrodeposited metallic-sheet material; and 30-40 mesh glass beads. Various wick compositions and water levels were investigated.

Vapor bubble migrations within the wick material influenced the performance of the apparatus. Providing a means for vapor escape improved the performance considerably. As a result, performance could be improved by using wick materials having larger mesh openings. Sintering screen samples to the boiler surface to reduce contact resistance did not improve performance.

TABLE OF CONTENTS

I.	INTRODUCTION -----	9
A.	BACKGROUND -----	9
B.	OBJECTIVE -----	10
II.	EXPERIMENTAL DESIGN -----	11
III.	EXPERIMENTAL PROCEDURE -----	25
IV.	RESULTS AND DISCUSSION -----	28
V.	CONCLUSIONS -----	45
VI.	RECOMMENDATIONS FOR FURTHER STUDY -----	46
APPENDIX A	THERMOCOUPLE CALIBRATION DATA -----	47
APPENDIX B	SAMPLE CALCULATIONS -----	50
APPENDIX C	UNCERTAINTY ANALYSIS -----	54
APPENDIX D	LEAST SQUARES METHOD FOR OBTAINING T_w -----	57
APPENDIX E	PREPARATION OF NICKEL SCREEN SAMPLES -----	60
BIBLIOGRAPHY	-----	61
INITIAL DISTRIBUTION LIST	-----	63
FORM DD 1473	-----	65

LIST OF TABLES

1.	Summary of Nickel Screen Characteristics -----	21
2.	Summary of Experimental Runs -----	29

Blank

P. 6

LIST OF FIGURES

1.	Photograph of boiler apparatus with screen sample in place -----	12
2.	Sectional view of boiler apparatus -----	13
3.	Overall view of experimental apparatus -----	14
4.	Photograph of nickel cylinder -----	17
5.	Top view of boiler apparatus -----	20
6.	Photograph of nickel screen sizes used in this investigation -----	23
7.	Determination of heat loss -----	31
8.	Comparison of pool boiling results -----	32
9.	Effect of pool depth -----	34
10.	Effect of aging on boiler surface -----	35
11.	A comparison of pool boiling with four layers of 80 mesh at various conditions -----	37
12.	Effect of wick height -----	39
13.	Effect of vapor bubble escape -----	40
14.	A comparison of mesh sizes -----	42
15.	A comparison of glass bead performance -----	43
16.	Thermal conductivity of nickel "A" -----	53
17.	Temperature profile in nickel cylinder -----	58

ACKNOWLEDGEMENTS

The author is deeply indebted to Dr. P. J. Marto for his continual advice, encouragement and interest as thesis advisor. Sincere appreciation is also due to Dr. P. F. Pucci for his helpful suggestions for the initial design of this project and to Dr. M. D. Kelleher as departmental reader. To the Mechanical Engineering Machine Shop personnel, especially Mr. George Baxter, to Mr. Robert C. Schiele, and to the Materials Science Laboratory personnel, the author expresses his gratitude for their efforts in constructing the components of the apparatus.

I. INTRODUCTION

A. BACKGROUND

The heat pipe, an efficient means of transporting large quantities of thermal energy, had its beginnings in a principle formulated by Gaugler in 1942 [1]* and developed independently by Grover in 1964 [2]. Essentially, a heat pipe consists of a closed container, usually cylindrical, whose walls are lined with a porous wick material leaving a vapor space in the center of the container. The wick is saturated with the working fluid which is vaporized by a heat source at the evaporator end. The vapor travels through the vapor space to the heat sink where it is condensed in the wick. The condensate is returned to the evaporator by capillary action and the cycle continues. The heat pipe contains no moving parts and is not affected by gravity; as a result, space applications are numerous.

Since its early development, numerous investigations of heat pipe parameters have been undertaken. These investigations have generally focused their attention on wick geometry, wick characteristics, performance characteristics and working fluids with the emphasis on liquid metals. A summary of the literature up to March 1968 has been compiled by Cheung [3].

Because of the flexibility of its components, primarily the working fluid and wick material, the heat pipe can be operated over a wide range of temperatures and pressures. Recent investigators have studied the major limitations of heat

*Numbers in brackets refer to references listed in Bibliography.

pipe performance, namely, failure of the wick material to supply working fluid to the evaporator at high heat fluxes and boiling in the wick structure which impedes the flow of the working fluid. These limitations are directly related and dryout, characterized by high temperature gradients in the evaporator section, results. Kunz, et al. [4] investigated both limitations using a wick covered planar surface for their boiling studies, and concluded that high heat transfer coefficients and heat transfer rates can be obtained provided that the vapor can escape from the wick material. Mosteller [5], using a glass enclosed everted heat pipe, observed two types of boiling--a gentle form of boiling at higher pressures and a more vigorous boiling caused by dryout. Neither type appeared to effect heat pipe operation. Recent studies at North Carolina State University [6] have investigated the boiling mechanism using glass and monel beads as the wick material. As a result, heat transfer coefficients and critical heat fluxes can be predicted when the values of porosity, capillary rise and permeability of wick materials are known.

B. OBJECTIVE

The objective of this study was to systematically investigate nucleate boiling from mesh covered surfaces while simulating as closely as possible actual heat pipe operation. Various nickel screen sizes and water levels were studied.

II. EXPERIMENTAL DESIGN

FACTORS CONSIDERED AND CHOICE OF MATERIALS

The factors considered in the design of the boiling apparatus included simulating heat pipe operation as closely as possible, permitting visual observation of the boiling process, flexibility of operation and simplicity in design and construction. While satisfying the first three factors, the last was kept constantly in mind.

The final design of the boiler apparatus consisted of the following major components: a nickel cylinder whose top surface was the boiling surface; a cylindrical heater unit containing seven cartridge heaters; a glass containing ring to enclose the boiling area and the surrounding water; a phenolic base, mated to the glass ring, from which the nickel and copper cylinders were supported; a stainless steel top cap containing a glass viewport; a reflux condenser connected to the top cap; a 600 ml beaker to collect the condensate and act as a water reservoir; and a container to enclose the nickel and copper cylinders and the asbestos insulation. Figure 1 is a photograph of the boiler apparatus and Figure 2 is a sectional view.

A 0.5 inch high stainless steel ring to hold screen samples on the boiler surface and a 2 inch high stainless steel ring for pool boiling investigations were held in place by a stainless steel flange and three stainless steel set screws. Both rings were machined so that the inner edges did not touch the actual boiling surface. Instrumentation consisted of a variac to regulate the voltage input, a voltmeter, an ammeter, copper-

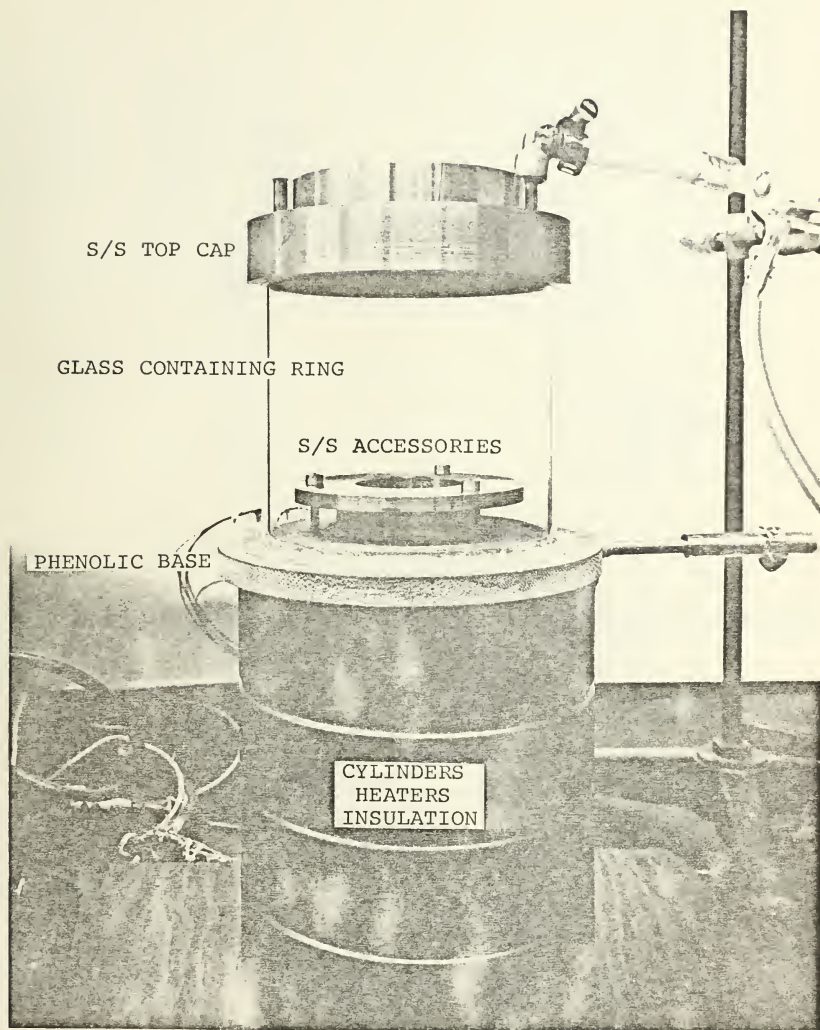


Figure 1. Photograph of Boiler Apparatus
With Screen Sample in Place.

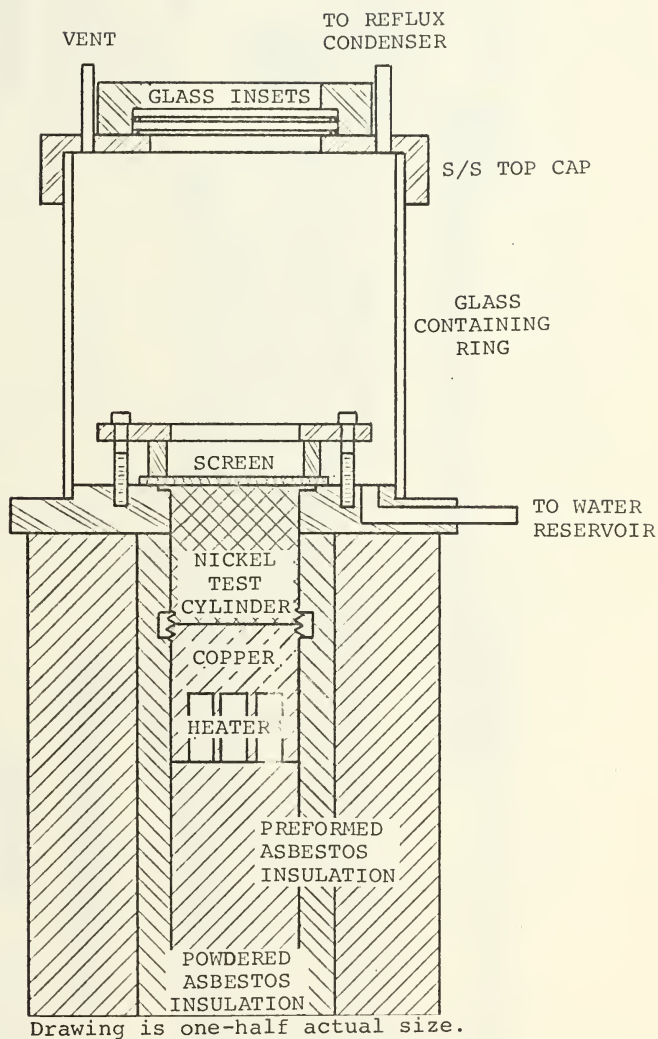


Figure 2. Sectional View of Boiler Apparatus.

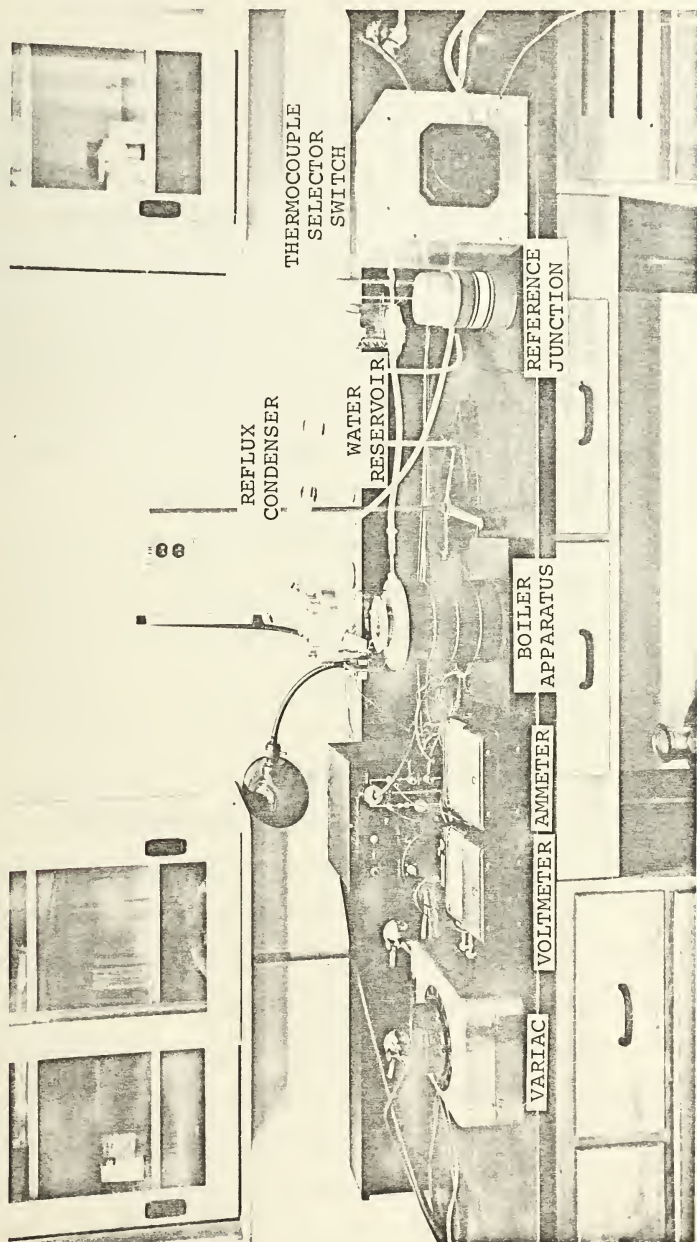


Figure 3. Overall View of Experimental Apparatus.

constantan thermocouples and a Hewlett-Packard Data Acquisition system. Figure 3 is an overall view of the experimental apparatus.

Previous studies of heat pipe operation at the Naval Postgraduate School [7,8] had used nickel pipe with nickel screen serving as the wicking material and for this reason, a nickel boiler surface was used. Nickel screen, fed by capillary action, was used as the wicking material. The glass containing ring and glass viewport in the top cap, permitted visual observation during actual runs provided the following procedures were carried out. A flow of hot air was directed : on the glass ring in the vicinity of the area to be observed, eliminating condensation on the glass. To permit visualization through the top cap, a resistance wire heater was wound on the cap and connected to a variac. These procedures enabled observation of the apparatus at all times.

The stainless steel accessories were readily accessible and as a result, screen samples could be changed with relative ease. By using stainless steel, the risk of corrosion and contamination of the distilled water was markedly reduced. Disassembling of the entire apparatus and changing boiler surfaces could be accomplished within two hours.

Copper was chosen for the heater cylinder because of its high thermal conductivity and the ease with which the heaters could be inserted into the cylinder.

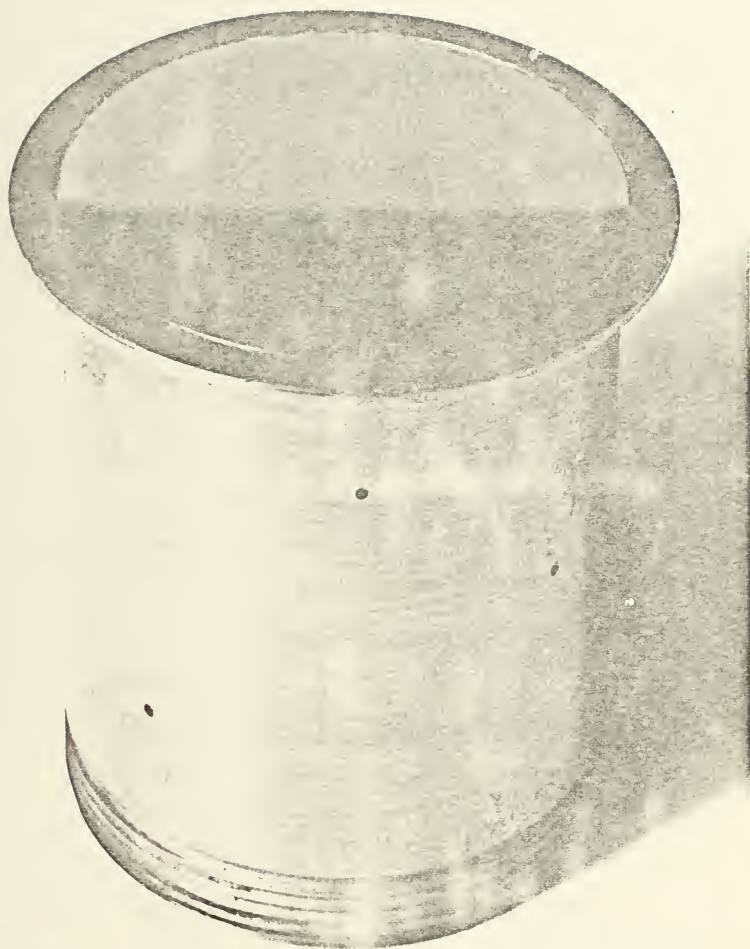
A detailed description of the components is contained in the following section.

COMPONENTS

The nickel cylinder was machined from a 2-1/2 inch Nickel 200 rod to a 1.875 inch diameter. Nickel 200, formerly designated "A" nickel, is 99.46% pure nickel and for a given temperature, its thermal conductivity can be obtained from experimental data [9]. A 0.1875 inch lip, 0.050 inch thick, extended from the sides of the cylinder, 0.010 inch from the boiling surface itself; the lip was undercut until the final thickness at the machined diameter of the cylinder was 0.015 inch. (See Figure 4). The bottom of the lip provided a means of supporting the heater-boiling surface assembly from the phenolic base while the undercutting reduced the extent of conduction losses through the lip. Two nickel cylinders were machined, both at an overall height of 2 inches with the bottom 0.25 inch threaded.

In order to ensure that the boiling surfaces of the nickel cylinders were smooth and uniform, the surfaces were polished using Buehler Metallurgical Polishing Equipment. The polishing procedure consisted of using three polishing wheels and polishing solutions consecutively and repeating the procedure until the surfaces were uniform. The polishing wheels and solutions listed in increasing fineness were:

- 1) canvas polishing wheel and 500 carborundum-water solution
- 2) kitten-ear broadcloth polishing wheel and alumina powder-water solution



Cylinder is shown approximately twice actual size.

Figure 4. Photograph of Nickel Cylinder.

- 3) AB Rayvel polishing wheel and gamma alumina-water solution.

When the surfaces were considered uniform, they were roughened slightly using No. 240 Three-M-Itte Elek-Tro-Cut cloth to promote nucleate boiling.

Six 0.040 inch holes, 0.625 inch deep were drilled in the nickel cylinder to accomodate the thermocouples. Four holes were drilled at ninety degree angles to each other, 0.5 inch below the boiling surface. The fifth hole was drilled 1 inch below the surface and the last hole was drilled 1.5 inches below the surface. No two holes lay in the same plane parallel with the longitudinal axis of the cylinder. The first four were placed in a plane perpendicular to the axis to determine if the temperature distribution throughout the nickel was uniform. (Figure 4).

As a base for the boiling apparatus and as a support for the nickel cylinder, phenolic was chosen for its low thermal conductivity, low porosity and high machinability. The 1.875 inch hole in the center of the 6.5 inch phenolic disk was counterbored 0.050 inch so that the actual boiling surface would sit slightly higher than the phenolic surface. Three threaded holes were drilled into the top surface of the base to accommodate the stainless steel set screws which would hold the screen samples in place.

The 2 inch high copper heater unit was machined to a diameter of 1.875 inches, was threaded at the top and had seven

0.375 inch holes, 1 inch deep, drilled into the bottom. Watlow Firerod cartridge heaters, 0.375 inch in diameter, 1 inch long and having a capacity of 150 watts each, were inserted into the holes. The bottom surface of the nickel cylinder and the top surface of the copper were polished until uniform, then coated with Silver Goop to ensure good contact and to prevent sticking after heating. A threaded nickel ring held the two cylinders in direct contact.

After assembly, the cylinders were covered with one inch thick preformed asbestos insulation around which powdered asbestos was packed. The lower portion of the apparatus, i.e. cylinders and insulation, was contained in a 6 inch diameter can.

A stainless steel ring, 0.5 inch high with outer diameter 2.5 inches and inner diameter 2 inches, was placed on top of the screen samples so that its inner edge lay above the lip of the nickel cylinder. A similar ring 2 inches high and grooved at its bottom surface was used to obtain pool boiling data. These rings were held in place by the stainless steel flange and set screws. Figure 5 is a top view of the boiler apparatus with an 80 mesh screen sample in place.

The screen samples were cut from commercially available nickel wire cloth. Some of the samples were cut from Lektro-mesh, a one-piece electrodeposited metallic-sheet material made of pure nickel having no overlapping wires and with both surfaces smooth. Table 1 lists the characteristics of the

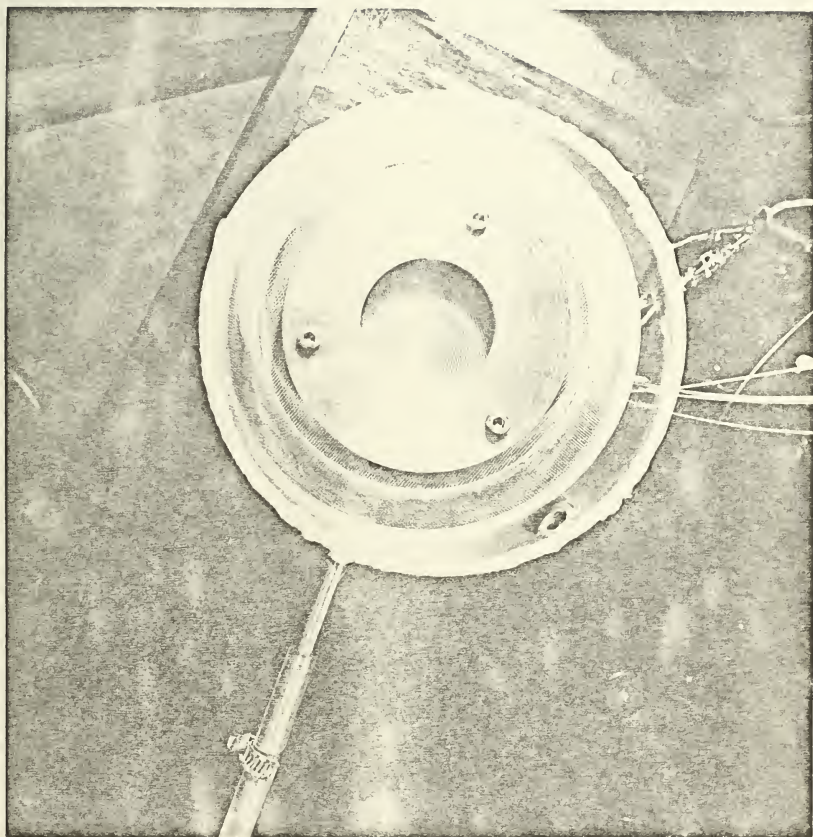


Figure 5. Top View of Boiler Apparatus.

TABLE 1
SUMMARY OF SCREEN SAMPLE CHARACTERISTICS

<u>SCREEN</u>	<u>WIRE DIAMETER</u>	<u>SPACE OPENING</u>	<u>% OPEN AREA</u>
50 mesh	0.009 "	0.0134 "	35.3
80 mesh	0.007 "	0.0055 "	19.4
150 mesh	0.0026 "	0.0041 "	37.4

<u>LEKTROMESH</u>	<u>LAND WIDTH</u>	<u>HOLE SIZE</u>	<u>% OPEN AREA</u>
100 count	0.006 "	0.004 "	16.0

various screen samples. Figure 6 is a photograph of the four types of screen samples used in this study. Preparation of the screen samples is covered in Appendix E.

Several runs were made with 30-40 mesh glass beads as the wick material. The beads were separated into sizes using U.S. standard sieves. Prior to use in the apparatus, the beads were washed in a warm cleaning solution and boiled for one hour in distilled water. The beads were placed within the 0.5 inch stainless steel ring directly on the boiling surface and confined by a piece of 50 mesh screen between the flange and the 0.5 inch ring.

The glass containing ring, five inches in outer diameter, mated with the phenolic base and was sealed with a silicone rubber sealant. The silicone rubber proved to be an excellent seal yet its easy removal permitted rapid disassembly of the apparatus.

Glass inserts in the stainless steel top cap permitted visual observation from above. The cap could be vented to the atmosphere or connected to the reflux condenser, which used tap water as the coolant. The condensate was collected in a 600 ml beaker and returned to the system via a supply hole in the phenolic base.

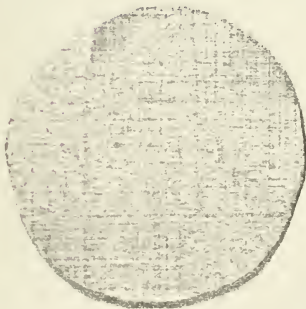
A variac was used to control the voltage input to the heaters and the power input was determined with a voltmeter and ammeter. Copper-constantan thermocouples were considered most appropriate in this investigation and six 0.040 inch type-T, metallic sheathed thermocouples were inserted into the



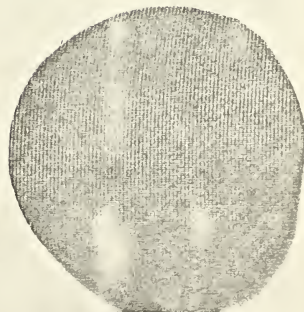
100 COUNT
LEKTROMESH



50 MESH



150 MESH



80 MESH

Figure 6. Photograph of Nickel Screen Sizes
Used In This Investigation.

nickel cylinder to a depth of 0.625 inch. The thermocouples were wired to a thermocouple selector switch and read with the Hewlett-Packard Model 2010C Data Acquisition System containing a guarded data amplifier and an integrating digital voltmeter.

III. EXPERIMENTAL PROCEDURE

To insure that experimental conditions were uniform prior to each data-taking run, the following procedures were carried out. The Data Acquisition System required a warmup time of one and one half hours before reliable data could be obtained. In order to save time and to prevent any malfunction caused by repeated start-up and securing of the equipment, the System was left operating the entire data-taking period. As a result, only a minor calibration, zeroing of the apparatus, was required prior to each run. The ice bath reference junction was prepared and the voltmeter and ammeter were checked for proper connections and zero reading.

Acetone was used to clean the boiler surface and all stainless steel parts to be used in the data-taking run. A thorough rinsing with distilled water followed to remove all traces of the acetone. Distilled water was also used to clean the glass ring to permit maximum visual observation.

For those runs using the nickel screen, placement of the appropriate layers of screen in a random orientation directly on the boiler surface followed. For runs without screen, the 2 inch stainless steel ring was placed directly on the lip of the nickel cylinder leaving the boiler surface exposed. Distilled water was then added to the desired level and the system was ready for operation.

A "hot start" method of operation was employed to reduce the time involved in data taking. A heat flux corresponding to a 60 volt input (approximately 250 watts) was added and the

system allowed to boil for 15 minutes. The power was then secured and the system allowed to cool. When the thermocouple 1.5 inches above the heaters read less than +4.000 millivolts (approximately 200°F), the system was considered sufficiently cool.

The system was then considered ready for operation and the voltage was increased in 5-volt increments commencing with a 20-volt input. The thermocouples were read at the 5-volt increments. The maximum voltage input was 60 volts; however, the temperature of the hottest thermocouple (closest to the heaters) imposed the limitation that readings above +11.5 millivolts were not considered reliable since the temperature corresponding to that value was 10°C above the highest fixed temperature used in calibrating the thermocouples. At the start of a given run, the atmospheric pressure was recorded from an aneroid barometer and used to calculate the saturation temperature of the vapor. Data (voltage, current, thermocouple voltages) was obtained when steady state operation for a given heat flux was reached. This was assumed to be the point at which the voltage of the thermocouple closest to the heater was increasing at a rate less than 0.005 millivolts per minute. This assumption meant that the temperature was essentially constant for a period of at least 5 minutes, and appeared valid since at 212°F a one degree increase in temperature corresponds to a voltage increase of 0.026 millivolts for copper-constantan thermocouples, while at 450°F a one degree increase in

temperature corresponds to a voltage increase of 0.031 millivolts. For most of the data taken, the voltage increase was less than 0.005 millivolts per minute.

In addition to the data mentioned above, the apparatus was monitored closely and significant occurrences and visual observations were noted on the data sheet.

IV. RESULTS AND DISCUSSIONS

Pool boiling data was obtained first to compare the operation of the boiler apparatus with previous results. Four types of nickel screen and glass beads were then investigated as the wick materials at various water levels and wick configurations. The results of all experimental runs are summarized in Table 2. The majority of the graphs show heat flux based on the temperature profile in the nickel cylinder plotted against the difference between the temperature at the boiling surface and the vapor saturation temperature.

The heat flux computed from the power input to the heaters was compared with the heat flux based on the temperature profile. In Figure 7, comparisons were made for several different conditions -- pool boiling, four layers of 80 mesh screen and eight layers of 80 mesh screen. The results were fairly consistent and indicate a heat loss of 16.67%.

Figure 8 compares pool boiling obtained with this apparatus with the Rohsenow correlation for water and nickel ($C_{sf} = 0.006$) [10], the pool boiling data from an Inconel flat plate of Kunz, et al. [4] and the pool boiling data from a square stainless steel surface of Alleavitch [6]. The closer correlation of the data to that of Alleavitch points up a similarity in basic design and water levels. This data was obtained at a water level of 1 inch while Alleavitch used a pool depth of 3 inches; the pool depth for the Kunz data was unknown but was assumed to be quite small.

TABLE 2

SUMMARY OF EXPERIMENTAL RUNS

<u>RUN</u>	<u>WICK MATERIAL/POOL BOILING</u>	<u>WATER DEPTH/REMARKS</u>
1	Pool boiling	5/8 inch, dryout permitted
2	Pool boiling	2 inches
3	Pool boiling	1 inch
4	Pool boiling	.067 inch (height of 4 layers 80 mesh), dryout permitted
5	4 layers 80 mesh	100% submergence (ratio of thickness of wick submerged to total thickness of wick) [4], dryout permitted
6	2 layers 80 mesh	1/2 inch above top layer
7	4 layers 80 mesh	100% submergence
8	4 layers 80 mesh	1/2 inch above top layer, boiler not disassembled prior to run
9	8 layers 80 mesh	100% submergence
10	4 layers 80 mesh hole in top layer	100% submergence
11	4 layers 80 mesh	100% submergence, top layer replaced, boiler surface not cleaned
12	4 layers 80 mesh hole in top 2 layers	100% submergence
13	4 layers 80 mesh hole in top 3 layers	100% submergence
14	4 layers 80 mesh hole in all layers	100% submergence
15	Pool boiling	1 inch
16	Pool boiling	1 inch
17	3 layers 50 mesh	100% submergence

<u>RUN</u>	<u>WICK MATERIAL/POOL BOILING</u>	<u>WATER DEPTH/REMARKS</u>
18	13 layers 150 mesh	100% submergence
19	3 layers 50 mesh	100% submergence
20	24 layers 100 count lektromesh	100% submergence
21	1/2 inch bed 30-40 mesh glass beads	2 inches above boiler surface
22	1/2 inch bed 30-40 mesh glass beads	100% submergence
23	4 layers 80 mesh sintered to boiler surface	100% submergence

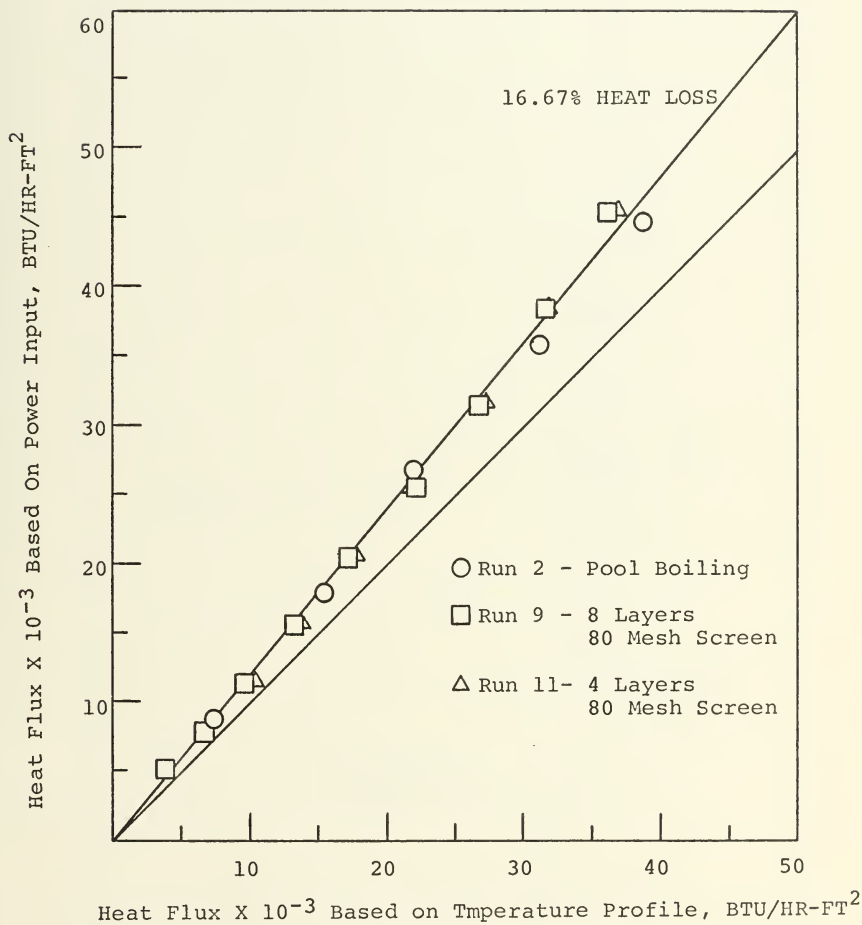


Figure 7. Determination of Heat Loss.

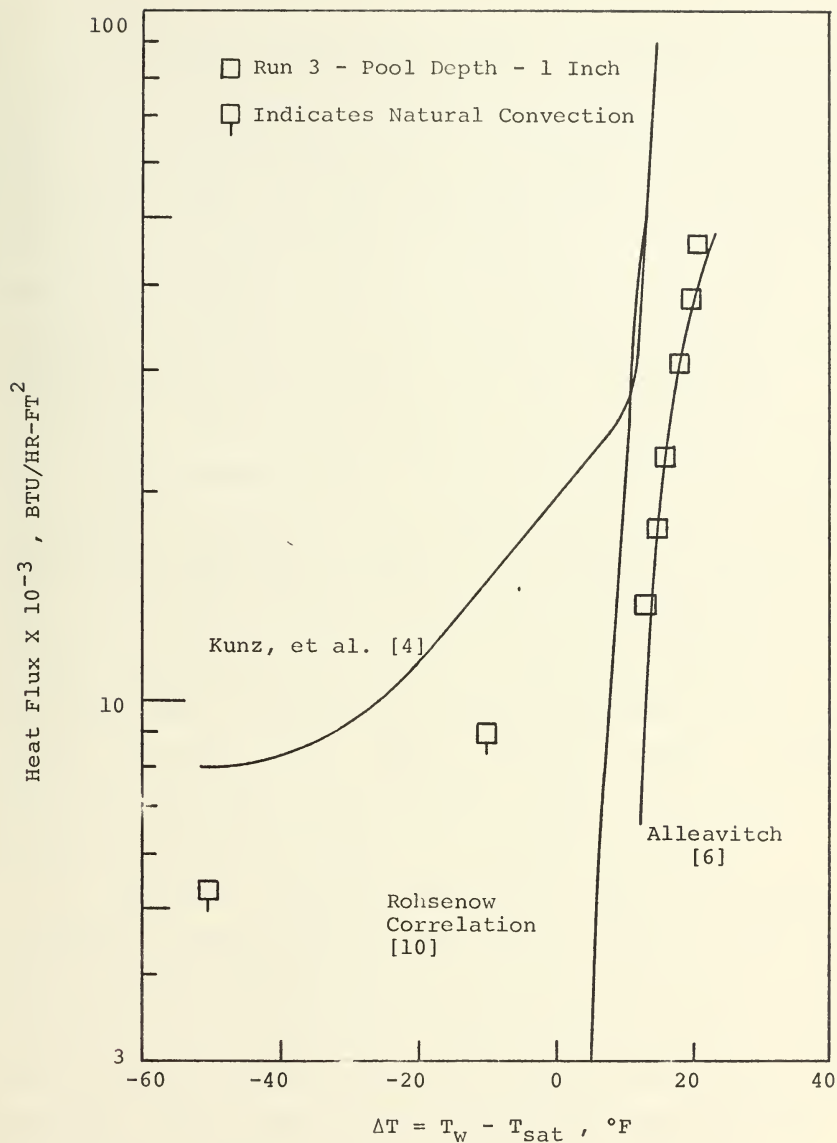


Figure 8. Comparison of Pool Boiling Results.

Pool boiling at three water levels was compared as shown in Figure 9 with dryout permitted at the lowest level, 0.067 inch. This height is equivalent to the height of four layers of 80 mesh screen. All data was taken with the 2 inch stainless steel ring in place which prevented any direct communication between the fluid above the boiling surface and the remaining fluid within the glass containing ring except at the feeding grooves at the bottom of the ring. Although not conclusive, in the natural convection area, pool depths of 1 and 2 inches provided better cooling than the 0.067 inch depth. Furthermore, a reduction in pool depth from 2 inches to 1 inch improved the performance slightly in the natural convection area. This could possibly be attributed to the formation of a more efficient controlled convective pattern within the 1 inch pool depth as opposed to a random fluctuating motion within the 2 inch pool depth. For the lowest pool depth, a temperature drop was noted prior to dryout, a fact also observed in a study of nucleate boiling at low liquid levels [11].

As expected, a definite aging effect caused by an oxide or chemical coating forming on the boiler surface was observed. Figure 10 shows the retardation of performance for Runs 3 and 16 under identical conditions. The data for Run 3 was obtained after 10 hours operation while that of Run 16 was obtained after 78 hours. For all runs, unless specifically noted otherwise, the surface had been cleaned of any detectable deposits.

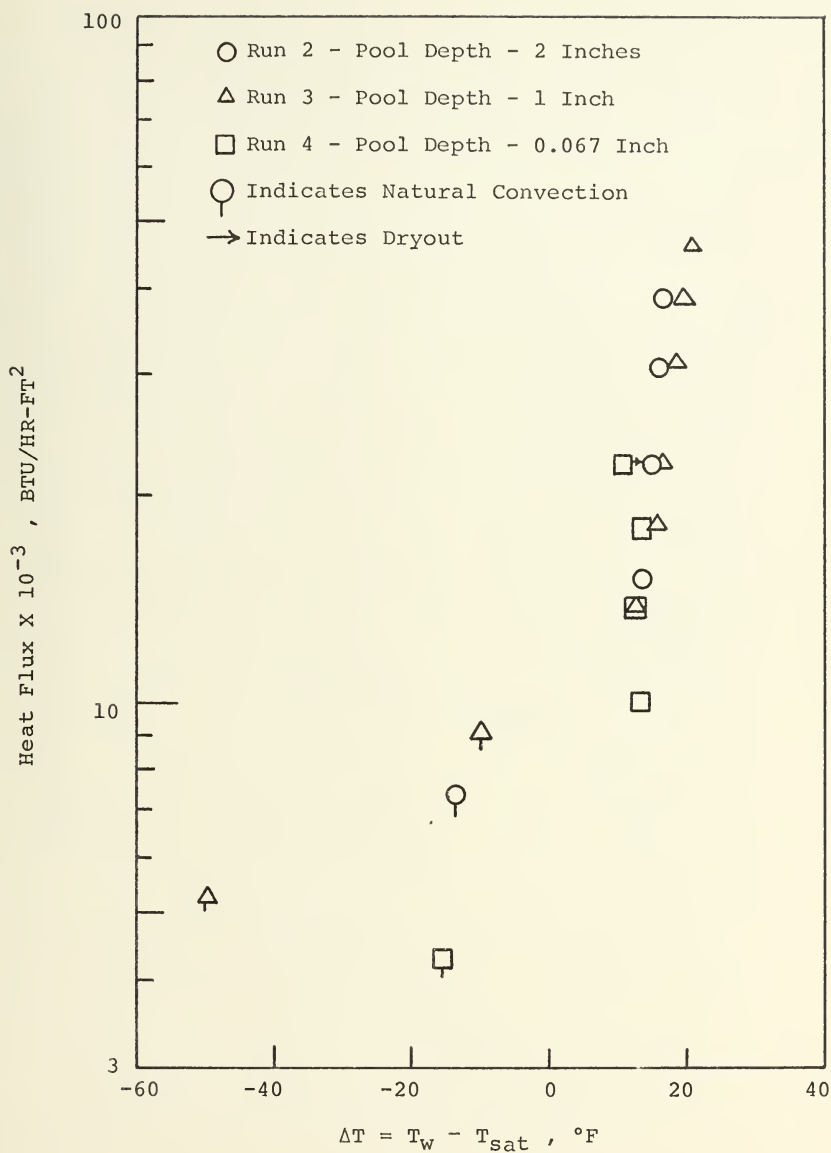


Figure 9. Effect of Pool Depth.

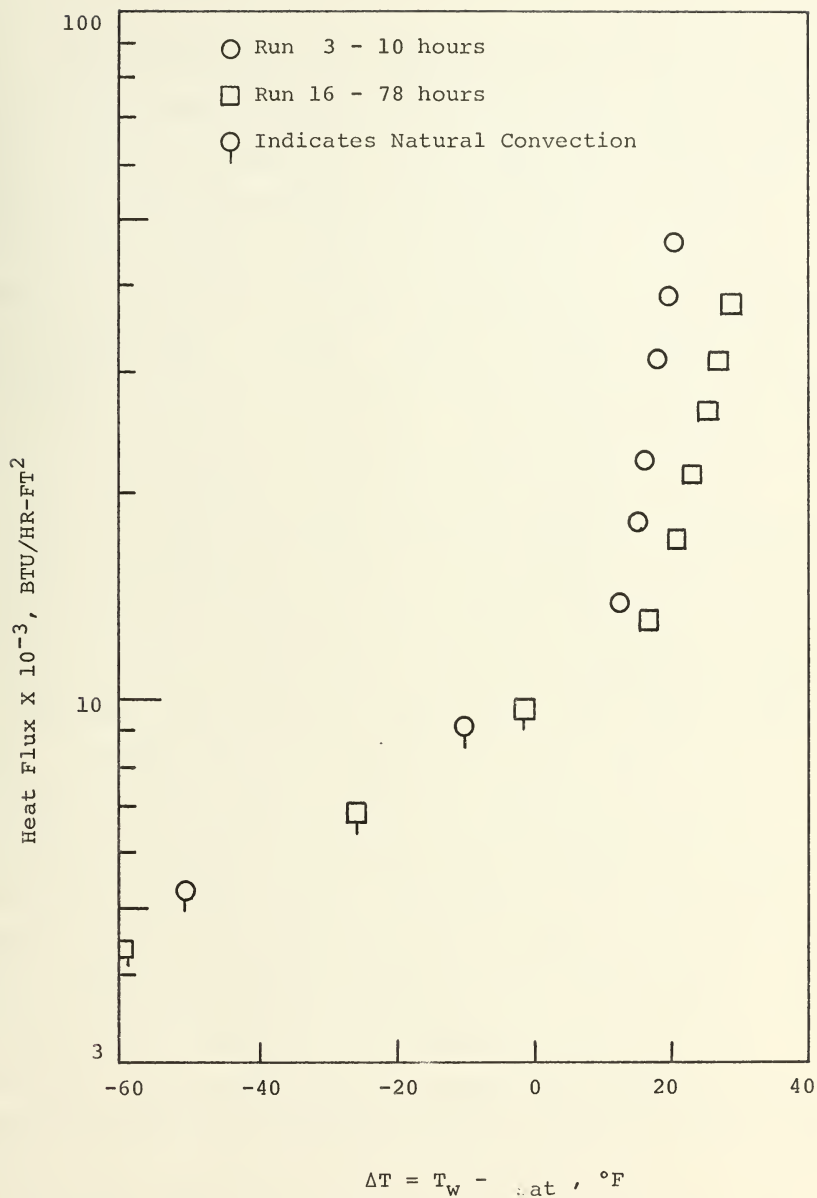


Figure 10. Effect of Aging on Boiler Surface.

Pool boiling for a pool depth equivalent to four layers of 80 mesh screen was compared with four layers under a variety of conditions in Figure 11. In all cases, the boiling data indicated that the presence of the wick material retarded performance. Runs 5, 7 and 11 were performed at 100% submergence, i.e., the water level was maintained at the level of the highest layer of screen. In Run 5, however, dryout was permitted. For Run 8, the water level was maintained 1/2 inch above the top layer of the screen. Four layers of 80 mesh screen were sintered to the surface of the second nickel cylinder in a Watkins Johnson hydrogen controlled atmosphere furnace for two hours at 1200°C. The sintering process was used to reduce the possibility of contact resistance and the results are plotted for Run 23. Despite a general similarity in operating conditions, the scattering of data was considerable. Possible causes for variations in the data could be attributed to the random orientation of the screen samples (no effort was made to standardize the orientation), contact resistance (although the poor performance with the sintered sample indicates that reducing contact resistance by sintering has no beneficial effect on performance), and the random nature of vapor bubble formations and migrations within the wick material. No conclusion could be made from a comparison of degree of submergence although this may also have affected the data.

A comparison of two layers of 80 mesh (Run 6) and four layers of 80 mesh (Run 8) with the water level 1/2 inch above

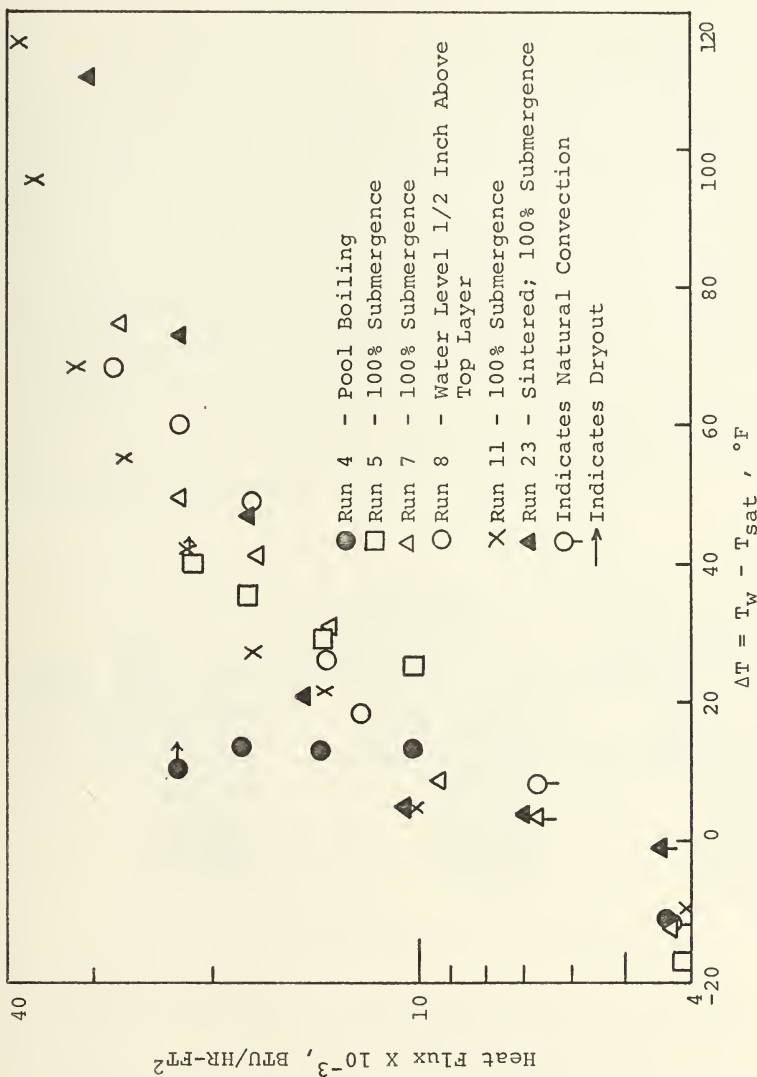
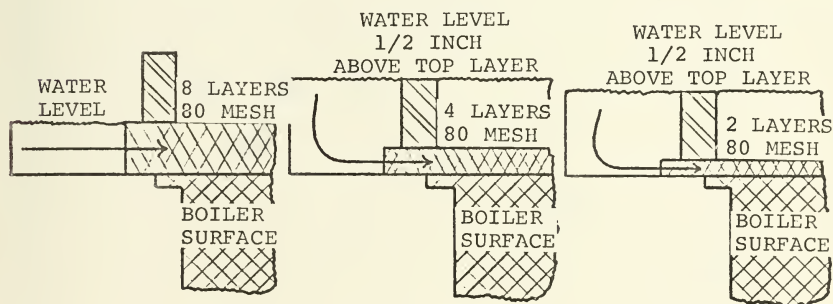


Figure 11. A Comparison of Pool Boiling With Four Layers of 80 Mesh At Various Conditions.

the top layer of screen and eight layers of 80 mesh at 100% submergence is shown in Figure 12. With the wick composed of eight layers, relatively cool water was constantly being fed from the water reservoir into the area surrounding the boiling area and subsequently fed into the wick. For the cases of four layers and two layers, the amount of water surrounding the boiling area was considerably larger, and as a result, was heated prior to being fed into the wick. (See figure below.) The addition of the warmer water resulted in higher temperature differences.



Data was obtained for Runs 10, 12 and 14 after drilling 1/8 inch holes in the centers of successive layers of screen. Figure 13 is a comparison of this data with previous data from Runs 7 and 11. The addition of the holes permitted vapor bubbles to escape and performance improved with the number of holes in the layers.

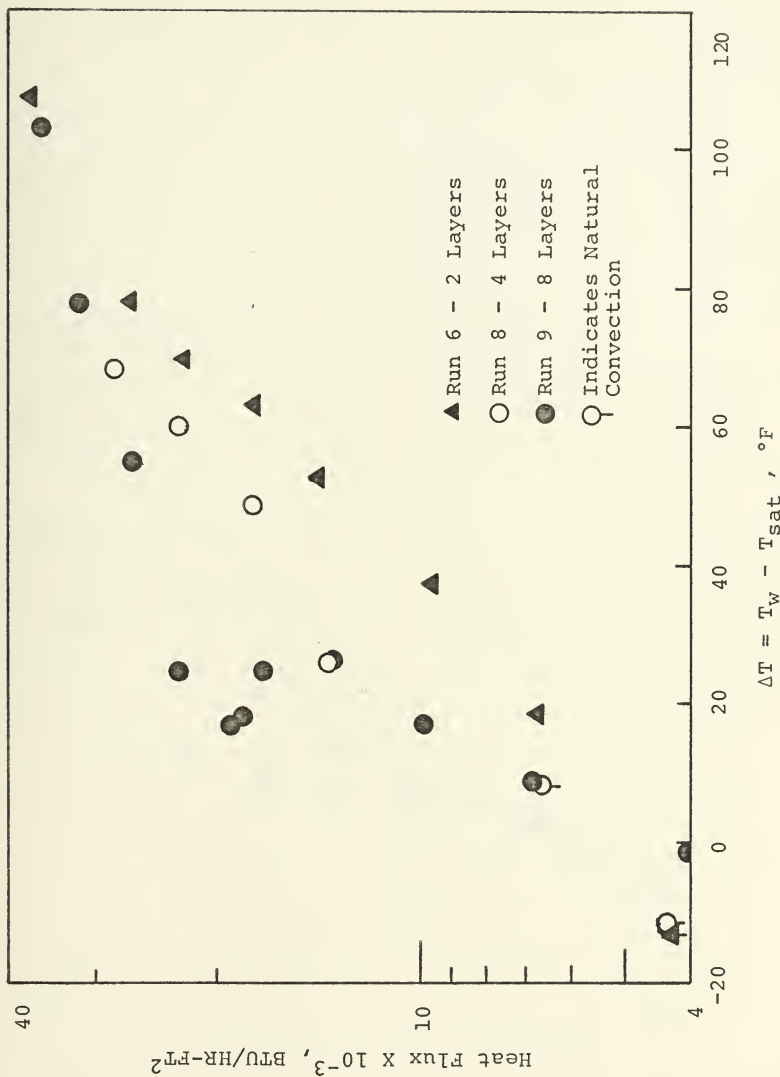


Figure 12. Effect of Wick Height.

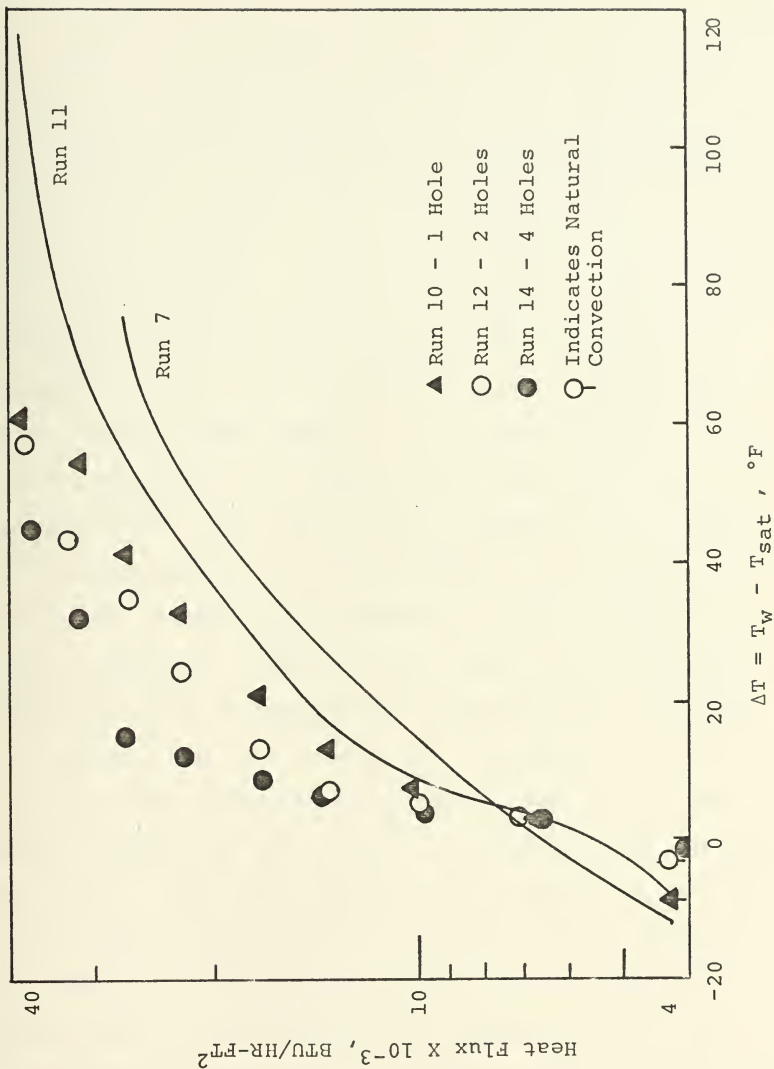


Figure 13. Effect of Vapor Bubble Escape.

Data for approximately equal heights of different size screens was compared with data from Runs 7 and 11 in Figure 14. Frequent vapor bubble passage through the 50 mesh screen was observed. In almost all other screen sizes, vapor bubble passage was through the edges of the layers. Vapor bubbles were observed moving across the top layer of the 50 mesh wick, indicating that the theory of vapor bubble migration was plausible. This type of movement was not observed with any of the other screen samples. As expected the performance with the 50 mesh screen was considerably better than any of the other samples. This data closely resembles that of pool boiling with a water level equivalent to four layers of 80 mesh. Due to small mesh openings of the 150 mesh and 100 count Lektromesh, little, if any, vapor bubble passage was permitted and high temperature differences were observed.

Glass beads were used as the wick material in Runs 21 and 22. The water level was maintained at two inches above the boiler surface for Run 21 while the wick was 100% submerged for Run 22. This data was compared in Figure 15 with that of Ferrell and Johnson [12] who performed similar experiments with the wick 100% submerged inclined at an angle of 1.3° . Visual observation of convective currents in the 2 inch water level indicated the addition of warmer water to the boiling area and consequently temperature differences were higher than those with 100% submergence. (See figure below.) Only 50 mesh nickel screen had slightly better performance than glass beads.

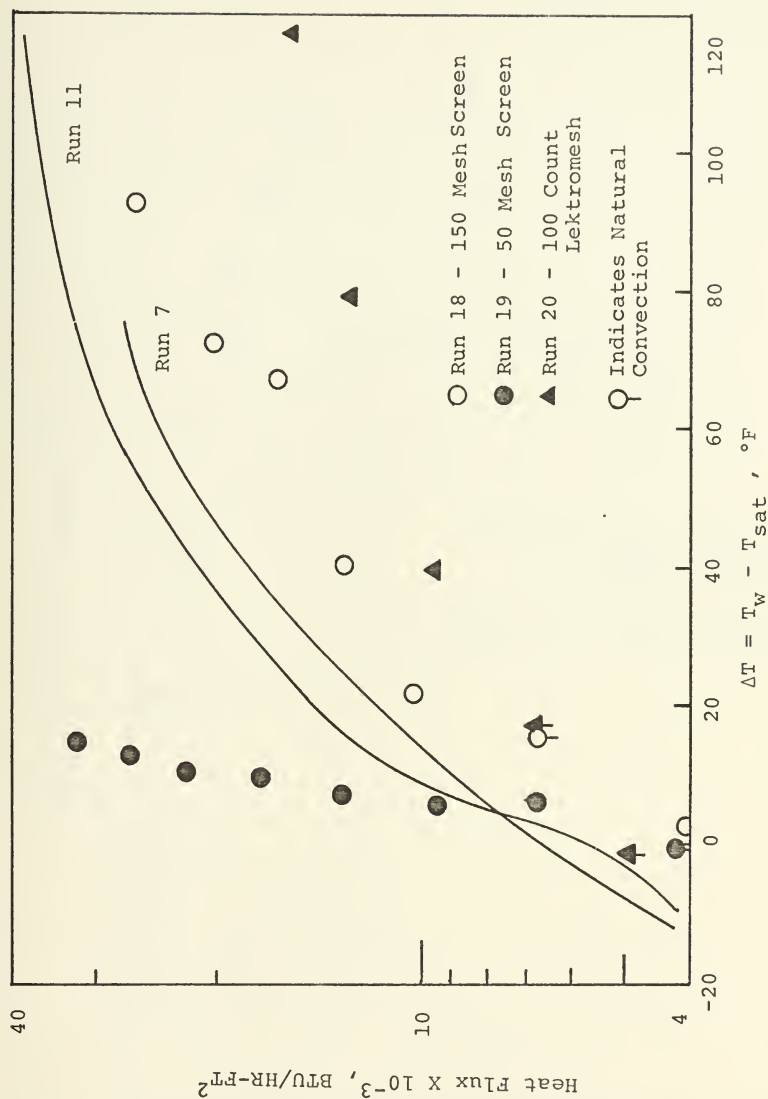


Figure 14. A Comparison of Mesh Sizes.

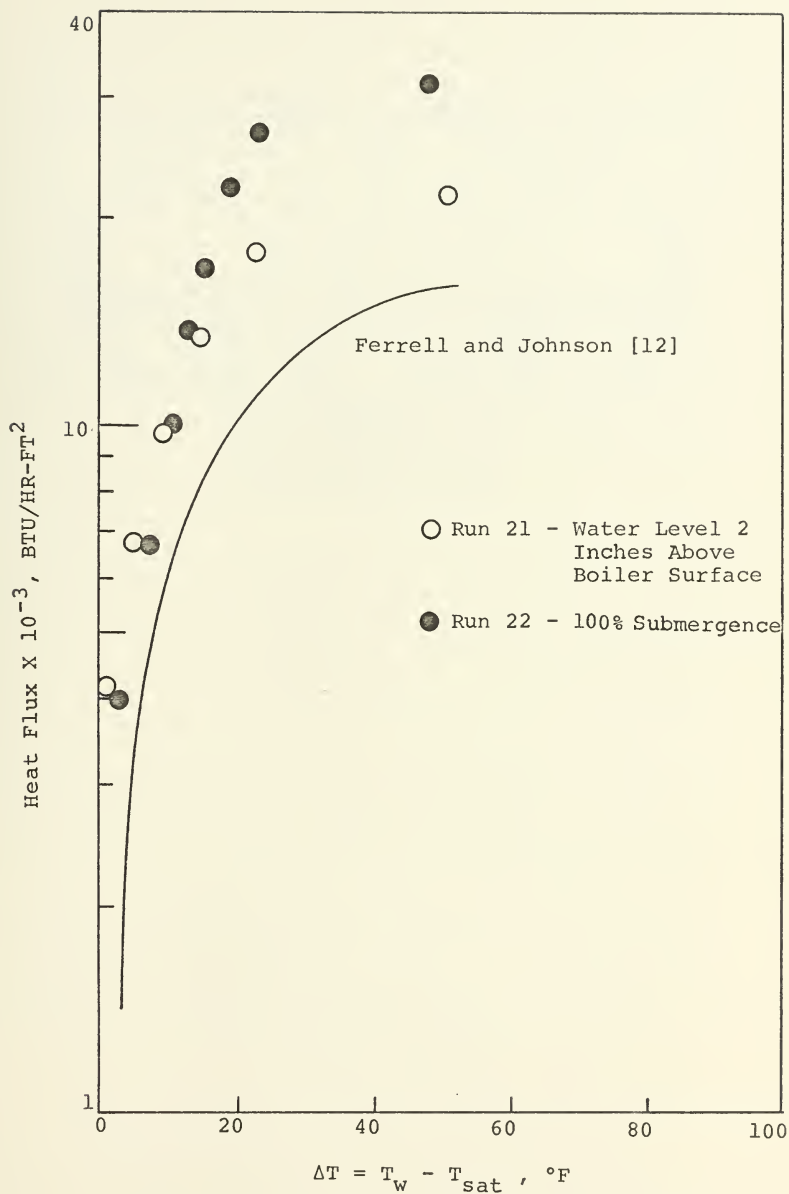
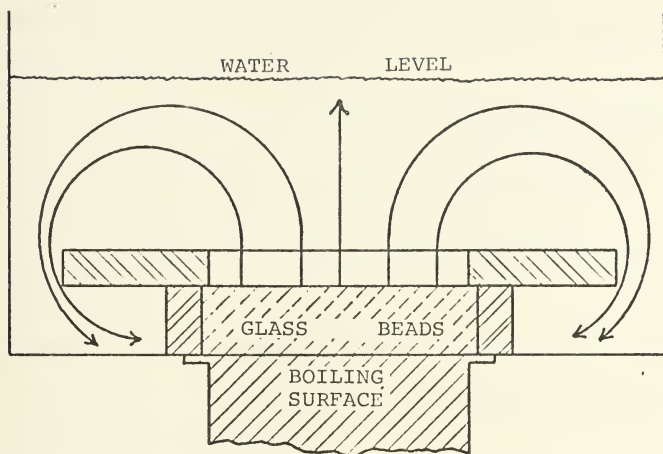


Figure 15. A Comparison of Glass Bead Performance.



V. CONCLUSIONS

1. The use of larger mesh sizes in the boiling apparatus improved the heat transfer.
2. The scattering of data obtained for similar conditions with the wick material present suggested the presence of a moving vapor pocket within the wick material.
3. Providing a means for vapor bubble escape improved performance.
4. Sintering screen samples to the boiler surface as described in Section IV in order to reduce contact resistance did not improve performance.
5. Glass beads as the wick material had better performance than all but the 50 mesh nickel screen wicks.

VI. RECOMMENDATIONS FOR FURTHER STUDY

1. Standardize screen orientation relative to mesh opening to determine its effect on performance.
2. Vary combinations of several screen sizes to determine optimum configuration for best performance.
3. Redesign feed mechanism to sense slight decreases in the height of the working fluid.
4. Increase size of screen samples to diameter equal to inside diameter of glass containing ring. Cool the glass ring, thereby allowing condensate to return to the wick directly for feeding into the boiling area. This would closely approximate actual heat pipe operation.

APPENDIX A

THERMOCOUPLE CALIBRATION DATA

Six metallic-sheathed copper-constantan thermocouples were inserted into the nickel cylinder to measure the temperature gradient and ultimately, through the use of the least squares method, to determine the temperature at the boiling surface. The properties of these particular metals proved them to be most suitable for the temperature range studied.

To insure accuracy in measurement, the thermocouples were calibrated at fixed reference points spanning the experimental temperature range. These fixed reference points included:

- 1) Melting point of ice -- 0°C (32°F)
- 2) Boiling point of water -- Dependent upon atmospheric pressure
- 3) Freezing point of pure tin -- 231.88°C (449.38°F)

All calibration voltages were measured with the reference junction in a distilled water-ice bath and read with a Hewlett-Packard Data Acquisition System Model 2010C containing a guarded data amplifier and an integrating digital voltmeter. The ice bath consisted of finely crushed ice made from distilled water in a Dewar flask and saturated with distilled water.

ICE POINT			
	Temperature	0°C (32°F)	
	Standard	0.000 millivolts	
<u>Thermocouple</u>	<u>Millivolts observed</u>		<u>Uncertainty</u>
1	+0.030		± 0.001 mv
2	+0.030		± 0.001 mv
3	+0.031		± 0.001 mv
4	+0.031		± 0.001 mv
7	+0.031		± 0.001 mv
8	+0.032		± 0.001 mv

Three determinations of voltages were made and the results averaged and listed in table above.

BOILING POINT		
	Pressure	759.5 mm Hg
	Temperature	99.98°C (211.97°F)
	Standard	+ 4.276 millivolts
<u>Thermocouple</u>	<u>Millivolts observed</u>	<u>Uncertainty</u>
1	+ 4.2945	± 0.0015 mv
2	+ 4.2965	± 0.0015 mv
3	+ 4.2975	± 0.0015 mv
4	+ 4.2945	± 0.0015 mv
7	+ 4.3020	± 0.0010 mv
8	+ 4.3010	± 0.0010 mv

To measure the boiling point of water, a stoppered 500 milliliter erlenmeyer flask, vented to the atmosphere and half-filled with distilled water, was heated until rapid boiling occurred. After allowing the distilled water to boil to remove entrapped air, the thermocouples were inserted through the stopper to a point one inch above the boiling water. In this manner a valid reading of the vapor temperature was observed. Two determinations of voltages at the pressure given above were made and the results averaged and listed in the table above.

To calculate the equilibrium temperature of boiling water, the atmospheric pressure was recorded from an aneroid barometer and the following equation used:

$$T_p = 100 + 28.012 \left(\frac{P}{P_o} - 1 \right) - 11.64 \left(\frac{P}{P_o} - 1 \right)^2 + 7.1 \left(\frac{P}{P_o} - 1 \right)^3$$

where

T_p = equilibrium temperature in degrees C

P = local atmospheric pressure in mm Hg

P_o = standard atmospheric pressure in mm Hg [14]

MELTING POINT OF TIN

Temperature 231.88°C (from NBS sample)
Standard +11.012 millivolts

<u>Thermocouple</u>	<u>Millivolts Observed</u>	<u>Uncertainty</u>
1	+ 11.0100	± 0.0020 mv
2	+ 11.0150	± 0.0010 mv
3	+ 11.0070	± 0.0010 mv
4	+ 11.0085	± 0.0015 mv
7	+ 11.0240	± 0.0010 mv
8	+ 11.0140	± 0.0010 mv

To measure the tin point, a National Bureau of Standards tin sample (melting point - 231.88°C) was heated in a stoppered test tube placed in a Hoskins Electric Furnace. The thermocouple was inserted through the stopper into the molten tin to a depth of approximately 1-1/4 inches. Powdered graphite was sprinkled on the molten tin to retard oxidation. When the tin was thoroughly molten, the furnace was secured and the voltage of the molten tin monitored with the digital voltmeter until the freezing point was reached. The freezing point of tin was characterized by an almost constant voltage (read every 0.1 second) for a period of approximately five minutes.

Using the voltages obtained for the three fixed reference points to solve for the three unknown constants (APPENDIX B), the following equation was used to determine a table of temperature-voltage relations for each thermocouple:

$$E = A + BT + CT^2 \quad [13, 14]$$

APPENDIX B

SAMPLE CALCULATIONS

1. Thermocouple Calibration (thermocouple #1)

The voltages corresponding to the three fixed reference points have been determined in Appendix A. The constants, A, B, and C in the equation

$$E = A + BT + CT^2 \quad (1)$$

are determined in the following:

- a) Ice point - temperature = 0.0°C , $E = 0.030$ mv.

Substituting these values in equation (1),

$$\begin{aligned} 0.03 &= A + B(0.0) + C(0.0)^2 \\ A &= 0.030 \end{aligned} \quad (2)$$

- b) Boiling point of water - temperature = 99.98°C ,

$E = 4.2945$ mv. Substituting again in (1),

$$\begin{aligned} 4.2945 &= 0.030 + B(99.98) + C(99.98)^2 \\ 4.2645 &= 99.98B + 9996.40C \end{aligned} \quad (3)$$

- c) Freezing point of tin - temperature = 231.88°C ,

$E = 11.0100$ mv.

$$\begin{aligned} 11.0100 &= 0.030 + B(231.88) + C(231.88)^2 \\ 10.980 &= 231.88B + 53768.334C \end{aligned} \quad (4)$$

Using the Wang Calculator and carrying calculations to ten decimal places, equations (3) and (4) were solved simultaneously for C. This value was then substituted in equation (3) to solve for B. As a result,

$$B = 0.0390904262$$

$$C = 0.0000356290$$

and the equation for the voltage -temperature relationship now became,

$$E = 0.030 + 0.0390904262T + 0.000035629T^2 \quad (5)$$

A computer solution for voltages was obtained by solving equation (5) for every degree between 1°C and 249°C. Similar solutions were obtained for the remaining thermocouples.

2. Least Squares Method for Obtaining T_w (Example - Run 23 - 40 volt input)

With the necessary information from smooth data, the following sums are formed (APPENDIX D),

T_i	X_i	$i = 1, 2, 3$
322.25	0.5	
301.28	1.0	
280.11	1.5	
$\Sigma T_i = 903.64$	$\Sigma X_i = 3.0$	

$T_i X_i$	X_i^2
161.12	0.25
301.28	1.00
420.16	2.25
$\Sigma T_i X_i = 882.56$	$\Sigma X_i^2 = 3.50$

Substituting these values in the equations for D and F yields,

$$D = \frac{3 \Sigma X_i T_i - (\Sigma X_i)(\Sigma T_i)}{3 \Sigma X_i^2 - (\Sigma X_i)^2}$$

$$D = \frac{3(882.56) - 3.0(903.64)}{3(3.5) - 9} = \frac{63.24}{1.5} = -42.16$$

$$F = \frac{(\Sigma T_i)(\Sigma X_i)^2 - (\Sigma X_i T_i)(\Sigma X_i)}{3 \Sigma X_i^2 - (\Sigma X_i)^2}$$

$$F = \frac{903.64(3.5) - 882.56(3)}{3(3.5) - 9} = \frac{515.06}{1.5} = 343.37$$

As a result,

$$T = -42.16X + 343.37$$

and solving for the temperature at the surface,

$$T_w = -42.16(2.0) + 343.37 = 259.05^\circ\text{F}$$

3. Calculation of Heat Flux from Power Input (40.0 volt
2.82 amp input)

$$\frac{q}{A} = \text{Voltage} \times \text{Current} \times \frac{3.413 \text{ BTU}}{\text{HR} - \text{WATT}} \times \frac{4}{\pi D^2 \text{FT}^2}$$

$$\frac{q}{A} = \frac{40.0 \times 2.82 \times 3.413}{0.019} = 20,262.41 \frac{\text{BTU}}{\text{HR} - \text{FT}^2}$$

4. Calculation of Heat Flux from Temperature Profile (Example -
Run 23 - 40 volt input)

$$\frac{q}{A} = \frac{k(T_1 - T_{3\text{avg}})}{(X_3 - X_1)}$$

The thermal conductivity was obtained at the average
temperature over the interval $\frac{(T_1 + T_2 + T_{3\text{avg}})}{3}$ from the

curve plotted in Figure 16 from the following data:

Thermal Conductivity of Nickel 200 (formerly "A" Nickel)

[9]

$T^\circ\text{C}$	$T^\circ\text{F}$	$k \left(\frac{\text{BTU}}{\text{HR-FT-}^\circ\text{F}} \right)$
0	32	42.1
100	212	37.5
200	392	33.4
300	572	29.0
400	752	27.6

$$\frac{q}{A} = \frac{35.30 \text{ BTU} (372.25 - 280.11) ^\circ\text{F} \times 12 \text{ in}}{(\text{HR-FT-}^\circ\text{F}) \times 1 \text{ in} \times \text{FT}} = 17,850.50 \frac{\text{BTU}}{\text{HR-FT}^2}$$

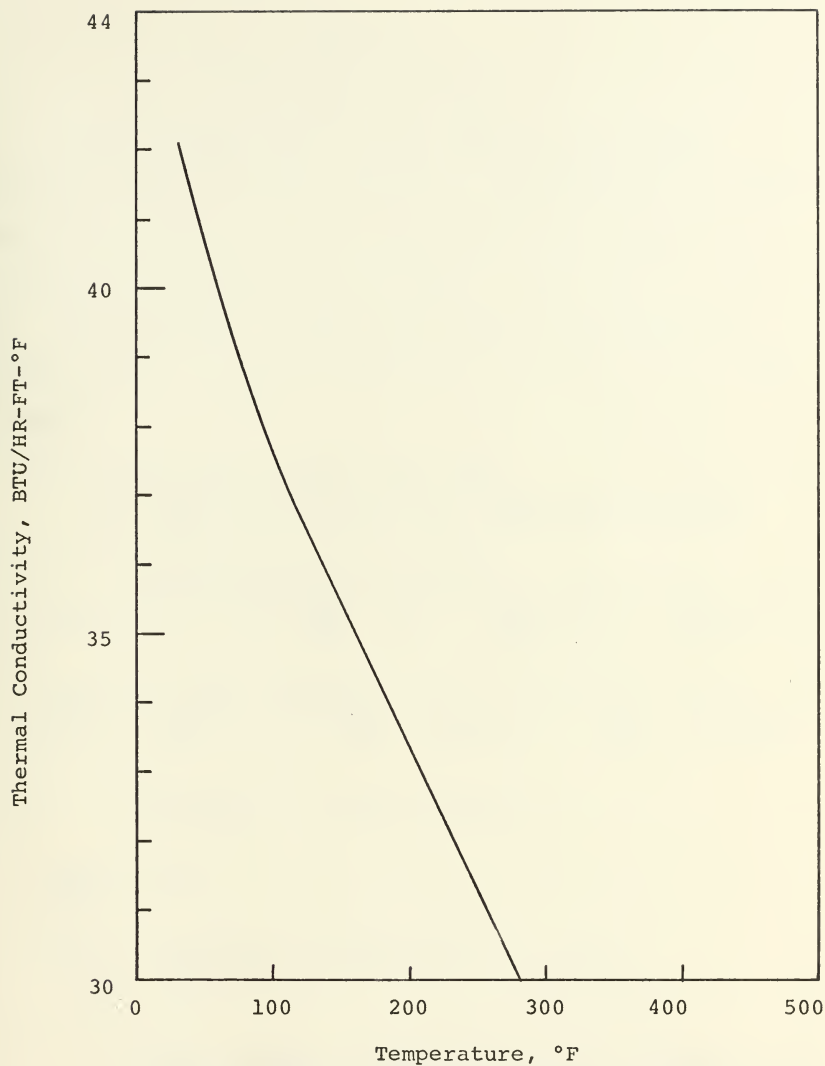


Figure 16. Thermal Conductivity of Nickel "A".

APPENDIX C

UNCERTAINTY ANALYSIS

In order to determine the magnitude of the largest possible error in the data presented, an uncertainty analysis was performed for several data points of Run 3. The method of Kline and McClintock was followed as shown in Reference [15]. Uncertainties in heat flux based on the temperature profile and the temperature difference, $\Delta T = T_w - T_{sat}$, were obtained.

A. Uncertainty in $\Delta T = T_w - T_{sat}$

1. Uncertainty in pressure reading from aneroid

barometer, $w_p = \pm 0.5 \text{ mm Hg}$

$$T_{sat} = 100 + 28.012 \left(\frac{P}{P_o} - 1 \right) - 11.64 \left(\frac{P}{P_o} - 1 \right)^2 + 7.1 \left(\frac{P}{P_o} - 1 \right)^3$$

$$\frac{\partial T_{sat}}{\partial P} = \frac{28.012}{P_o} - 23.28 \left(\frac{P}{P_o} - 1 \right) \left(\frac{1}{P_o} \right) + 21.3 \left(\frac{P}{P_o} - 1 \right)^2 \left(\frac{1}{P_o} \right)$$

for Run 3 $P = 763.5 \text{ mm Hg}$

$$\frac{\partial T_{sat}}{\partial P} = 0.04$$

$$w_{T_{sat}} = \frac{\partial T_{sat}}{\partial P} w_p = (0.04)(0.5) = \pm 0.02^\circ\text{C} \\ = \pm 0.04^\circ\text{F}$$

2. Uncertainty in interpolated values of temperature from calibration curves is $\pm 0.2^\circ\text{C}$ from Table 9 in Reference [14].

$$w_{T_w} = \pm 0.36^\circ\text{F}$$

3. As a result for the worst possible case, the uncertainty

$$\begin{aligned}w_{\Delta T} &= (w_{T_w} + w_{T_{sat}}) \\&= (0.36 + 0.04) = \pm 0.40^{\circ}\text{F}\end{aligned}$$

B. Uncertainty in heat flux

1. Uncertainty in reading k from Figure 15

$$w_k = \pm 0.05 \frac{\text{BTU}}{\text{HR-F}^{\circ}\text{F}}$$

2. Uncertainty in $(T_1 - T_{3\text{avg}})$ for the worst possible case

$$\text{let } T = (T_1 - T_{3\text{avg}})$$

$$\begin{aligned}w_T &= (w_{T_1} + w_{T_{3\text{avg}}}) \\&= (0.36 + 0.36) = \pm 0.72^{\circ}\text{F}\end{aligned}$$

3. Uncertainty in measuring distances = $\pm 0.0001\text{FT}$

$$\text{let } X = X_3 - X_1$$

$$\begin{aligned}w_X &= w_{X_3} + w_{X_1} \\&= 0.0001 + 0.0001 = \pm 0.0002\text{FT}\end{aligned}$$

4. For 34.80 volt input

$$\text{let } Q = \frac{q}{A}$$

$$Q = \frac{kT}{X}$$

$$\frac{\partial Q}{\partial k} = \frac{T}{X} = \frac{31.89}{.0833} = 382.83$$

$$\frac{\partial Q}{\partial T} = \frac{k}{X} = \frac{36.38}{.0833} = 436.73$$

$$\frac{\partial Q}{\partial X} = \frac{-kT}{X^2} = -\frac{(36.38)(31.89)}{(.0833)^2} = -168,139.13$$

$$w_Q = \left[\left(\frac{\partial Q}{\partial k} w_k \right)^2 + \left(\frac{\partial Q}{\partial T} w_T \right)^2 + \left(\frac{\partial Q}{\partial X} w_X \right)^2 \right]^{1/2}$$

$$w_Q = [(382.83 \times 0.05)^2 + (436.73 \times 0.72)^2 + (-168,139.13 \times 0.0002)^2]^{1/2}$$

$$w_Q = \pm 316.82 \frac{\text{BTU}}{\text{HR-FT}^2}$$

5. For 52.00 volt input

$$w_Q = \pm 316.82 \frac{\text{BTU}}{\text{HR-FT}^2}$$

6. For 64.00 volt input

$$w_Q = \pm 324.59 \frac{\text{BTU}}{\text{HR-FT}^2}$$

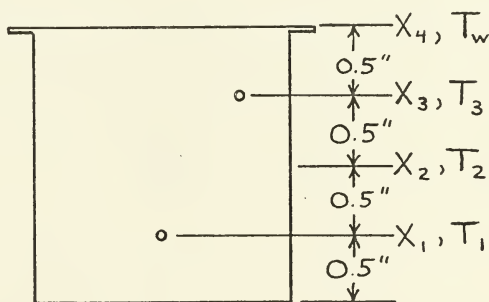
APPENDIX D

LEAST SQUARES METHOD FOR OBTAINING T_w

From Figure 17 (data extracted from Run 11) which is a plot of temperature profiles, the temperature is seen to vary linearly with position from the surface of the nickel cylinder. Taking advantage of this linearity, the method of least squares was used to predict the temperature of the boiler surface, T_w . An equation of the form

$$T = D X + F$$

was required to obtain T_w .



With the axis of the coordinate system at the bottom of the nickel cylinder, the following values were determined by the measurement of thermocouple positions.

$$X_1 = 0.5 \text{ in.}$$

$$X_2 = 1.0 \text{ in.}$$

$$X_3 = 1.5 \text{ in.}$$

$$X_4 = 2.0 \text{ in.}$$

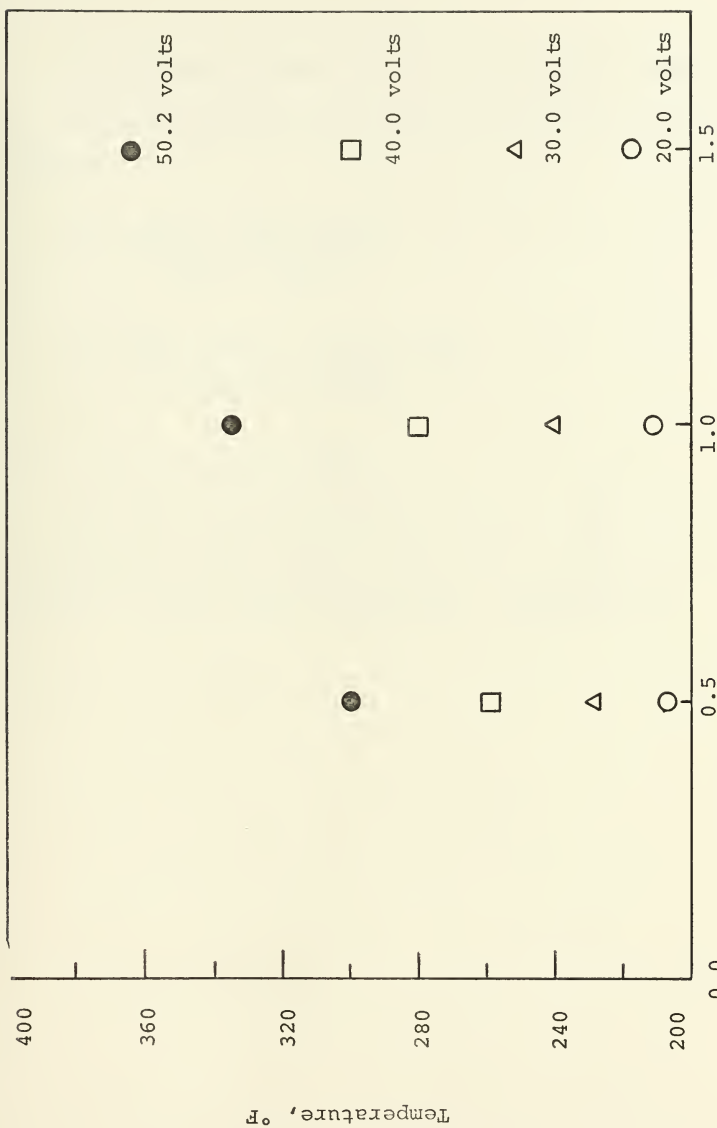


Figure 17. Temperature Profile in Nickel Cylinders.

Having these values and the corresponding temperatures, the following equations were used to determine the constants D and F:

$$D = \frac{3\sum X_i T_i - (\sum X_i)(\sum T_i)}{3\sum X_i^2 - (\sum X_i)^2}$$

$$F = \frac{(\sum T_i)(\sum X_i^2) - (\sum X_i T_i)(\sum X_i)}{3\sum X_i^2 - (\sum X_i)^2}$$

where $i = 1, 2, \text{ and } 3$ [15]

With the constants determined for a given power input and the distance to the surface known, the temperature at the surface, T_w , was easily determined. (APPENDIX B)

APPENDIX E

PREPARATION OF NICKEL SCREEN SAMPLES

After cutting the nickel screen to a diameter of 2-3/4 inches, the samples were placed in a Crest Ultrasonic Cleaner for twenty minutes in #222 L & R Waterless Ultrasonic Instrument Cleaning Solution. The samples were then rinsed in L & R Rinsing Solution. Subsequent rinsing in acetone and thorough flushing with distilled water prepared the samples for thermal oxidation as suggested by Kunz, et al [4]. Thermal oxidation causes the formation of nickel oxide on the screen which, having a smaller contact angle than pure nickel, increases the wettability of the nickel screen sample. The nickel screen samples were oxidized for a period of two hours at a temperature of 500°F in a Lindberg Hevi-duty Electric Furnace. After cooling, the samples were stored in plastic bags until used.

BIBLIOGRAPHY

1. Eastman, G. Y., "The Heat Pipe," Scientific American, pp.38-46, May 1968.
2. Grover, G. M., Cotter, T. P. and Erickson, G. F., "Structures of Very High Thermal Conductance," Journal of Applied Physics, v. 35, pp.1990-1991, 1964.
3. Lawrence Radiation Laboratory, University of California, Livermore, UCRL - 50453, A Critical Review of Heat Pipe Theory and Applications, by H. Cheung, 15 July 1968.
4. Lewis Research Center, NASA CR-812, Vapor - Chamber Fin Studies, Transport Properties and Boiling Characteristics of Wicks, by H. R. Kunz, L. S. Langston, B. H. Hilton, S. S. Wyde, and G. H. Nashick, June 1967.
5. Mosteller, W. L., The Effect of Nucleate Boiling on Heat Pipe Operation, M.S. Thesis, Naval Postgraduate School, Monterey, California, 1969.
6. Alleavitch, J., Vaporization Heat Transfer From Flooded Wick Covered Surfaces, Ph.D. Thesis, North Carolina State University, Raleigh, North Carolina, 1969.
7. Kilmartin, H. E., Jr., The Effect of Wick Geometry on the Operation of a Longitudinal Heat Pipe, M.S. Thesis, Naval Postgraduate School, Monterey, California, 1969.
8. Hickox, O. J., Jr., A Study of Wire Mesh Wick Characteristics in a Longitudinal Heat Pipe, M.S. Thesis, Naval Postgraduate School, Monterey, California, 1969.
9. Hogan & Sawyer, Journal of Applied Physics, 23, 177 (1952).
10. Rohsenow, W. M., and Choi, H. Y., Heat, Mass and Momentum Transfer, p.225, Prentice-Hall, Englewood Cliffs, New Jersey, 1961.
11. Nishikawa, K., Kusuda, H., Yamasaki, K., Tanaka, K., "Nucleate Boiling at Low Liquid Levels," Trans. Japan Society of Mechanical Engineers, v. 10, No. 38, pp.328-38, 1967.
12. Ferrell, J. K., and Johnson, H. R., The Mechanism of Heat Transfer in the Evaporator Zone of a Heat Pipe, ASME Paper No. 70-HT/SPT-12, Presented at ASME Space Technology and Heat Transfer Conference, Los Angeles, California, 21-24 June 1970.
13. Roeser, W. F., and Lonberger, S. T., "Methods of Testing Thermocouples and Thermocouple Materials," pp.235-1 to

255-21, Precision Measurement and Calibration, National Bureau of Standards, U.S. Government Printing Office, 1968.

14. Weber, R. L., Heat and Temperature Measurement, p. 63, Prentice-Hall, Inc., New York, 1950.
15. Holman, J. P., Experimental Methods for Engineers, pp.37-40, pp.61-64, McGraw-Hill, New York, 1966.

INITIAL DISTRIBUTION LIST

	No. Copies
1. Defense Documentation Center Cameron Station Alexandria, Virginia 22314	2
2. Library, Code 0212 Naval Postgraduate School Monterey, California 93940	2
3. Professor P. J. Marto Mechanical Engineering Department Naval Postgraduate School Monterey, California 93940	1
4. Professor P. F. Pucci Mechanical Engineering Department Naval Postgraduate School Monterey, California 93940	1
5. LT F. C. Gregory, USN Boston Naval Shipyard Boston, Massachusetts 02129	1

DOCUMENT CONTROL DATA - R & D

(Security classification of title, body of abstract and indexing annotation must be entered when the overall report is classified)

1. ORIGINATING ACTIVITY (Corporate author)		2a. REPORT SECURITY CLASSIFICATION	
Naval Postgraduate School Monterey, California 93940		Unclassified	
		2b. GROUP	
3. REPORT TITLE			
An Investigation of Nucleate Boiling From Mesh Covered Surfaces			
4. DESCRIPTIVE NOTES (Type of report and, inclusive dates)			
Master's Thesis; June 1970			
5. AUTHOR(S) (First name, middle initial, last name)			
Francis Carl Gregory			
6. REPORT DATE		7a. TOTAL NO. OF PAGES	7b. NO. OF REFS
June 1970		63	15
8a. CONTRACT OR GRANT NO.		9a. ORIGINATOR'S REPORT NUMBER(S)	
b. PROJECT NO.			
c.		9b. OTHER REPORT NO(S) (Any other numbers that may be assigned this report)	
d.			
10. DISTRIBUTION STATEMENT			
This document has been approved for public release and sale; its distribution is unlimited.			
11. SUPPLEMENTARY NOTES		12. SPONSORING MILITARY ACTIVITY	
		Naval Postgraduate School Monterey, California 93940	
3. ABSTRACT			
<p>A boiler apparatus, designed to simulate heat pipe operation, was built and used to investigate nucleate boiling at atmospheric pressure from mesh covered surfaces using distilled water as the working fluid. The wick materials used included 50 mesh, 80 mesh, and 150 mesh nickel screen; 100 count Lektromesh, a one-piece electrodeposited metallic-sheet material; and 30-40 mesh glass beads. Various wick compositions and water levels were investigated.</p> <p>Vapor bubble migrations within the wick material influenced the performance of the apparatus. Providing a means for vapor escape improved the performance considerably. As a result, performance could be improved by using wick materials having larger mesh openings. Sintering screen samples to the boiler surface to reduce contact resistance did not improve performance.</p>			

Thesis
G759
c.1

Gregory

118934

An investigation of
nucleate boiling from
mesh covered surfaces.

Thesis
G759
c.1

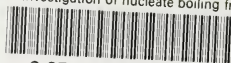
Gregory

118934

An investigation of
nucleate boiling from
mesh covered surfaces.

thesG759

An investigation of nucleate boiling fro



3 2768 002 13909 9

DUDLEY KNOX LIBRARY